



Acromyrmex leaf-cutting ants have simple gut microbiota with nitrogen-fixing potential

Sapountzis, Panagiotis; Zhukova, Mariya; Hansen, Lars H.; Sørensen, Søren Johannes; Schiøtt, Morten; Boomsma, Jacobus Jan

Published in:
Applied and Environmental Microbiology

DOI:
[10.1128/AEM.00961-15](https://doi.org/10.1128/AEM.00961-15)

Publication date:
2015

Document version
Publisher's PDF, also known as Version of record

Citation for published version (APA):
Sapountzis, P., Zhukova, M., Hansen, L. H., Sørensen, S. J., Schiøtt, M., & Boomsma, J. J. (2015). *Acromyrmex* leaf-cutting ants have simple gut microbiota with nitrogen-fixing potential. *Applied and Environmental Microbiology*, 81(16), 5527-5537. <https://doi.org/10.1128/AEM.00961-15>

Acromyrmex Leaf-Cutting Ants Have Simple Gut Microbiota with Nitrogen-Fixing Potential

Panagiotis Sapountzis,^a Mariya Zhukova,^{a,b} Lars H. Hansen,^c Søren J. Sørensen,^c Morten Schiøtt,^a Jacobus J. Boomsma^a

Centre for Social Evolution, Department of Biology, University of Copenhagen, Copenhagen, Denmark^a; Institute of Cytology and Genetics, Siberian Branch of the Russian Academy of Sciences, Novosibirsk, Russia^b; Molecular Microbial Ecology Group, Department of Biology, University of Copenhagen, Copenhagen, Denmark^c

Ants and termites have independently evolved obligate fungus-farming mutualisms, but their gardening procedures are fundamentally different, as the termites predigest their plant substrate whereas the ants deposit it directly on the fungus garden. Fungus-growing termites retained diverse gut microbiota, but bacterial gut communities in fungus-growing leaf-cutting ants have not been investigated, so it is unknown whether and how they are specialized on an exclusively fungal diet. Here we characterized the gut bacterial community of Panamanian *Acromyrmex* species, which are dominated by only four bacterial taxa: *Wolbachia*, *Rhizobiales*, and two *Entomoplasmatales* taxa. We show that the *Entomoplasmatales* can be both intracellular and extracellular across different gut tissues, *Wolbachia* is mainly but not exclusively intracellular, and the *Rhizobiales* species is strictly extracellular and confined to the gut lumen, where it forms biofilms along the hindgut cuticle supported by an adhesive matrix of polysaccharides. Tetracycline diets eliminated the *Entomoplasmatales* symbionts but hardly affected *Wolbachia* and only moderately reduced the *Rhizobiales*, suggesting that the latter are protected by the biofilm matrix. We show that the *Rhizobiales* symbiont produces bacterial NifH proteins that have been associated with the fixation of nitrogen, suggesting that these compartmentalized hindgut symbionts alleviate nutritional constraints emanating from an exclusive fungus garden diet reared on a substrate of leaves.

Communities of gut bacteria play key roles in nutrient acquisition, vitamin supplementation, and disease resistance. Their diversity often covaries with host diet, both across lineages with different ecological niches and between conspecific populations in different habitats or geographic regions (1–3). Elucidating the significance of single bacterial taxa in omnivores such as humans is dauntingly complex (3, 4), but insects with specialized diets have regularly offered gut microbiota study systems that are dominated by a limited number of species (5–7). Several insect-microbial symbioses are evolutionarily ancient so that extensive functional complementarity between hosts and symbionts could evolve, as in aphids that rely on *Buchnera* for the production of essential amino acids (8, 9). Other mutualisms have more recent origins, such as bedbugs that rely on *Wolbachia* for vitamin B production (10, 11) or wood-eating beetles that carry nitrogen-fixing gut bacteria in order to subsist on protein-poor diets (12).

The eusocial insects offer abundant niche space for bacterial symbionts (5, 13–16) because many have peculiar diets and practice liquid food transfer (trophallaxis), which facilitates symbiont transmission within colonies. Higher termites replaced their ancestral protist gut communities by bacterial microbiota (17), while other early studies identified *Blochmannia* gut symbionts in carpenter ants (18, 19) and a community of gut-pouch symbionts in *Tetraponera* ants (20, 21). More recently, comparative studies have started to survey the total complexity of the gut microbiota of ants to reveal overall nutritional adaptations associated with predatory and herbivorous feeding habits (6, 14, 19), and comparable studies in termites documented the importance of gut microbes for the conversion of dead plant material into nutrients that can be absorbed (22–24). A similar approach has been successful in honeybees and bumblebees and revealed microbiotas dominated by rather few bacterial species, consistent with bees having more predictable pollen and nectar diets than ants and termites, which have generalist feeding ecologies (5, 25–28).

The dominant gut bacteria of bees first appeared to be primarily adaptive in providing hosts with partial protection against gut parasites, but evidence for nutritional supplementation has increasingly been found (25–27, 29).

Recent studies of the gut microbiota of fungus-growing termites offered remarkable confirmation of the putative association between simple diets and simple gut microbiota, as it appeared that foragers consuming leaf litter and wood have complex microbiotas, whereas a mature queen had a gut microbial community of strikingly low diversity consistent with an exclusive fungal diet (23). Because leaf-cutting ants consume mostly if not exclusively fungus, we would thus expect to find a simple microbiota reminiscent of the microbial diversity in the guts of bees, who also have specialized diets (pollen and nectar). Because pollen is rather protein rich (30) relative to leaves (31), we would expect the leaf-cutting ant microbiota to have a higher likelihood of providing nutritional supplementation. This hypothesis is reinforced by a study that identified *Klebsiella* and *Pantoea* nitrogen-fixing bacte-

Received 30 March 2015 Accepted 30 May 2015

Accepted manuscript posted online 5 June 2015

Citation Sapountzis P, Zhukova M, Hansen LH, Sørensen SJ, Schiøtt M, Boomsma JJ. 2015. *Acromyrmex* leaf-cutting ants have simple gut microbiota with nitrogen-fixing potential. *Appl Environ Microbiol* 81:5527–5537. doi:10.1128/AEM.00961-15.

Editor: P. D. Schloss

Address correspondence to Panagiotis Sapountzis, sapountzis@bio.ku.dk, or Jacobus J. Boomsma, jiboomsma@bio.ku.dk.

Supplemental material for this article may be found at <http://dx.doi.org/10.1128/AEM.00961-15>.

Copyright © 2015, American Society for Microbiology. All Rights Reserved. doi:10.1128/AEM.00961-15

The authors have paid a fee to allow immediate free access to this article.

ria in the fungus gardens of *Atta* leafcutter ants, but without investigating their gut bacterial communities (32).

We tested these expectations in *Acromyrmex* leaf-cutting ants. Using 16S-454 and 16S-Miseq sequencing, we determined the major bacterial operational taxonomic units (OTUs) (representing a cluster of bacterial 16S rRNA gene sequences of $\geq 97\%$ similarity, typically interpreted as representing a bacterial species) associated with the digestive system of these ants. We then used a combination of fluorescence microscopy and electron microscopy to investigate the localization of the major bacterial OTUs across gut tissues, the lumen, and the surrounding fat bodies to make inferences about their putative adaptive roles. We subsequently kept ants on sterile sugar solutions with and without the antibiotic tetracycline and monitored changes in the prevalence of dominant gut bacteria. Finally, we focused on an extracellular *Rhizobiales* species that was restricted to the hindgut lumen and discovered that these bacteria are embedded in a biofilm-like matrix of polysaccharides and produce NifH proteins, which are known to mediate the reduction of free nitrogen to the bioavailable NH_3 .

MATERIALS AND METHODS

Ant collection and maintenance, sterile diets, DNA extractions, 454 pyrosequencing, and Illumina Miseq sequencing. Ant colonies were collected in Gamboa, Republic of Panama. We used 11 *Acromyrmex* lab colonies for 454 sequencing (eight *A. echinator*, two *A. octospinosus*, and one *A. volcanus*) and 13 partly overlapping *Acromyrmex* colonies for Miseq sequencing: six new colonies (sampled both in the field and after being transferred to the lab) and seven lab colonies, more than 2 years after collection (six of them had already been sequenced with 454). This double procedure was chosen because we were seeking to verify that bacterial gut communities could be reproduced across sequencing platforms and to elucidate their susceptibility to changes in rearing conditions (field versus 3 months in the lab versus > 2 years in the lab). An overview of the sampling and experimental procedures is provided in Table S1 in the supplemental material. DNA for both 454 and Miseq sequencing was extracted with the same methods (see details below), and all lab colonies were maintained in rearing rooms at ca. 25°C and 70% relative humidity (RH) under a 12 h photoperiod.

The ant workers that were reared on artificial diets were collected from lab colony Ae150 and were picked from the fungus gardens with forceps and placed in groups of 15 in sterile petri dishes (90 by 15 mm), which had an inverted screw cap in the middle that served as liquid food vial. Control experiments used petri dishes with 15 workers across four basic feeding regimes, i.e., FG (fructose [5%, wt/vol] plus glucose [5%, wt/vol]), FGY (fructose [5%, wt/vol] plus glucose [5%, wt/vol] plus yeast extract [2%, wt/vol]), S₁ (sucrose [10%, wt/vol]), SY (sucrose [10%, wt/vol] plus yeast [2%, wt/vol]), and the antibiotic treatments used a fully comparable set of feeding regimes (FGT, FGYT, ST₁, and SYT) with 1 mg/ml tetracycline added. The S and ST treatments were duplicated (S₂ and ST₂) with 20 and 60 ant workers, respectively, and all diet components were dissolved in sterile distilled water and filter sterilized. For an overall idea of the experimental setup, see Fig. S1B to D in the supplemental material. Petri dishes were monitored every second day for ant mortality.

To obtain an estimate of the gut bacterial diversity of the ants on different diets without killing them, we collected fecal droplets once a week from 5 of the 15 workers from each group (days 7, 14, 21, and 28) and stored them at -80°C until DNA extraction. Toward the end of the experiment (days 28 and 35), we dissected 2 to 5 living ants from each group (2 ants for each of the initial treatments [FG, FGY, S₁, SY, FGT, FGYT, ST₁, and SYT] and 5 ants from the duplicated treatments [S₂ and ST₂]), collected all gut tissues, and pooled them into single treatment and control samples per colony.

To obtain the DNA samples for 454 pyrosequencing, ant workers were anesthetized on ice, surface sterilized by submerging them into absolute

ethanol for 60 s, and then rinsed with sterilized distilled water. The ants were dissected in sterile phosphate-buffered saline (PBS) under a stereo microscope and stored at -80°C until DNA extraction. Five workers from each colony were dissected and all gut tissues collected, pooled in one sample, and frozen. All DNA samples were extracted from these frozen samples using the Qiagen blood and tissue kit following the manufacturer's instructions and including an extra step where glass beads of 0.5 mm were added and the lysate was vortexed for 30 s. All samples were reloaded in 150 μl AE elution buffer. Bacterial DNA amplification and 454 pyrosequencing were performed as described previously (33). Extracted DNA for the Miseq sequencing was sent to the Microbial Systems Laboratory at the University of Michigan for library preparation and sequencing.

Analyses of 454 and Miseq data. The 454 data were analyzed using mothur (v.1.33.3) (34) after nine rounds of filtering as described in the standard operating procedure (SOP) protocol with a few modifications (35) (page accessed July 2014): (i) sequences with homopolymer stretches longer than 10 bases were removed, (ii) the filtered sequences were aligned against the Silva 111 nonredundant database (36), and (iii) sequences were assigned to taxonomic groups using the Bayesian classifier implemented in mothur with a confidence threshold of 80% while using the same Silva database. In these filtering steps we also included the pre.cluster command, based on the algorithm developed by Huse et al. (37), and we removed all reads assigned to mitochondria, chloroplasts, *Archaea*, or *Eukaryota*. We did not exclude "unknown sequences" but did not find any either after the classification was completed. Operational taxonomic units (OTUs) were obtained by generating a distance matrix with pairwise distance lengths smaller than 0.15. The data were then clustered, and each OTU was classified with a 97% similarity cutoff using the same databases as before.

Rarefaction tables were constructed with mothur using pseudoreplicate OTU data sets containing between 1 and 13,927 sequences with 1,000 iterations per pseudoreplicate, and the curves were visualized in Microsoft Excel 2013. The final OTU table was rarefied at 5,800 reads and used for all downstream analyses, including the calculation of Euclidean distances that were used for principal-coordinate analysis (PCoA) in R. The read counts of the four most abundant OTUs were transformed to percentages, entered into JMP 10.0, and used to perform nonparametric Spearman tests for correlations that could suggest mutual exclusiveness or reinforcement.

For the Miseq data analysis, we also used mothur (v.1.33.3) (34) and performed several rounds of filtering as described in the SOP protocol (38) (page accessed October 2014), with the only difference being that sequences were assigned to taxonomic groups using the Bayesian classifier implemented in mothur with a confidence threshold of 80%. The final OTU table was rarefied at 28,000 reads and used for all downstream analyses, including the calculation of Euclidean distances that were used for PCoA in R. We used an analysis of variance (ANOVA) regression to correlate Miseq relative abundances with quantitative PCR (qPCR) absolute gene copy numbers for a random selection of samples (see below).

We retrieved OTU sequences from both data sets using python scripts and compared them to each other and to specific probes using the BLAST algorithm with a $1e-50$ E value cutoff and 50% identity (39). In order to design primers and probes from the retrieved OTUs, sequences were aligned using the Map to Reference algorithm incorporated in Geneious software v4.8.5 and v7.0.6 (40).

For the ant survival analyses, we used Cox proportional hazards models (with censoring), carried out with the coxph function of the Survival package of R (version 3.1.1), following assessment of proportional hazards using cox.zph (41, 42). The cofactors included the substrate, the presence of yeast, or the presence of tetracycline. Data were plotted using the survival analysis function in JMP 10.0. Effects of the different components of the diets on the presence/absence of certain bacterial groups in the guts and the fecal droplets were compared using pairwise multivariate

correlations across all samples. We constructed 2-by-2 contingency tables examining each of the bacterial species and diet components and evaluated their distribution frequencies using Pearson χ^2 tests in JMP 10.0. To validate bacterial presence in fecal droplets, we collected samples from the ants in experimental petri dishes at days 7, 14, 21, 26, and 28 and used a Cox proportional hazard model (with censoring) to analyze the data under the assumption that the number of days of bacterial survival in guts as sampled from fecal droplets was equal to the number of days of obtaining positive bacterial signals by dissections during the 4 weeks of monitoring (see Fig. S1C in the supplemental material). The diet groups that had positive bacterial signals in the fecal droplets until the last day of monitoring were considered censored.

PCRs. To identify *nifH* sequences, we used a previously described protocol (14) and sequences identified in colony Ae150 (accession number KP256164) to design *nifH*-specific primers (C8_nifH_F/R; see Table S3 in the supplemental material). These were then used either directly or to perform the second step of a nested PCR in combination with primers in the protocol described previously and targeting the same region (14, 32). PCR conditions were as follows: denaturation for 3 min at 94°C, followed by 40 cycles of 30 s at 94°C, 30 s at 60°C, and 30 s at 72°C and a 7-min final extension at 72°C. All PCR products were gel purified (QIAquick gel extraction kit [Qiagen] or Montage gel extraction kit [Millipore]) and sent to Eurofins (Germany) for sequencing. Samples with failing sequencing reactions or chromatographs with multiple peaks were reamplified and cloned using the TOPO TA cloning kit (Invitrogen). At least 20 bacterial colonies from each cloning were checked with PCR using the C8-nifH primers, and 10 positive PCR products from each cloning were sent to MWG for sequencing.

16S rRNA gene-specific primers were constructed in Geneious for *EntAcro1* (*Entomoplasmatales*), *RhiAcro1* (*Rhizobiales*), and *EntAcro2* (*Entomoplasmatales*) (see Table S3 in the supplemental material). The specificity of the primers was confirmed by PCR, cloning, and Sanger sequencing of various PCR products from different colonies, which showed that the primers amplify the expected sequences (data not shown). To detect *WolAcro1* (*Wolbachia*), we used the *wsp*-specific primers (43). PCR conditions were as follows: denaturation for 3 min at 94°C, followed by 35 cycles of 30 s at 94°C, 30 s at the annealing temperature (see Table S3 in the supplemental material), and 30 s at 72°C and a 7-min final extension at 72°C.

qPCR. A number of *A. echinator* colonies (four lab [>2 years] and two field) and *A. octospinosus* colonies (two lab [>2 years] and one field) were used to evaluate the accuracy of the relative abundances of the four major OTUs (*EntAcro1*, *EntAcro2*, *RhiAcro1*, and *WolAcro1*) obtained by 454 and Miseq sequencing. We targeted three out of the four major OTUs discovered in our study for which we had 16S rRNA gene-specific primers, i.e., Entom_F/Entom_A_R for *EntAcro1*, Entom_F/Entom_B_R for *EntAcro2*, and Phyllo_F/Phyllo_R for *RhiAcro1* (see Table S3 in the supplemental material) in reactions with SYBR Premix Ex Taq (TaKaRa Bio Inc., St. Germain en Laye, France) on the Mx3000P system (Stratagene, Santa Clara, CA, USA). Reactions took place in a final volume of 20 μ l containing 10 μ l buffer, 8.3 μ l double-distilled water (ddH₂O), 0.4 μ l of each primer (10 mM), 0.4 μ l ROX standard, and 0.5 μ l template DNA. PCR conditions were as follows: denaturation for 2 min at 94°C, followed by 40 cycles of 30 s at 94°C, 30 s at the annealing temperature (see Table S3 in the supplemental material), and 30 s at 72°C, followed by dissociation curve analysis. All quantitative PCRs (qPCRs) were replicated, and the cycle threshold (C_T) mean was used as a measure of relative gene abundance. Each run included two negative controls with no added template. All data were normalized relative to the ant EF-1 α gene as a control (44). For each gene that we analyzed, the initial template concentration was calculated from a standard curve with PCR product in 10-fold dilution series of known concentration, as quantified by NanoDrop. To evaluate whether the Miseq relative abundances correlated with the bacterial 16S rRNA gene copy numbers, we used ANOVA regression analysis in JMP 10.0.

FISH. Five to 10 ant workers from colony Ae150 for *A. echinator* and colony Ao492 for *A. octospinosus* were dissected in PBS, and their guts were placed in 4% paraformaldehyde and left for at least 24 h. For the permeabilization, deproteinization, and hybridization, we followed a previously described protocol (45). For the hybridization step, we used 0.75 μ g/ μ l specific labeled probes (see Table S3 in the supplemental material) targeting bacteria belonging to the class *Mollicutes* (order *Entomoplasmatales*) and the class *Alphaproteobacteria* (orders *Rhizobiales* and *Rickettsiales* [*Wolbachia*]). As negative controls, we used reverse probes for *Entomoplasmatales* and *Rhizobiales* (see Table S3 in the supplemental material), which gave faint diffuse signals in the fat bodies that probably originated from lipid droplets of significantly different size and intensity than the bacterium-specific signals (see Fig. S2 in the supplemental material). To check permeabilization of cell membranes, we used DAPI (4',6'-diamidino-2-phenylindole) staining as a positive control in each experiment because it has high cell permeability, and we thereby confirmed that our specific probes were able to cross cell membranes similarly to DAPI. We thus considered a signal as being specific when it was absent from the negative controls and colocalized with the DAPI bacterial staining. The fluorescent *in situ* hybridization (FISH) images were inspected and photographed using a Zeiss LSM 710 confocal microscope equipped with ZEN 2009 software and a Leica TCS SP2 microscope.

Immunofluorescence (IF) staining. Dissected tissues (digestive tract and fat body) of large workers were fixed in cold methanol (20 min, -20°C) and then permeabilized in cold acetone (5 min, -20°C). Samples were subsequently rinsed three times with PBS with 0.1% Triton X-100 (PBST) at room temperature (RT) and incubated for 5 min in PBST. This was followed by incubation of tissues for 1 h with 6 μ g/ml affinity-purified anti-NifH antibody (Agrisera, AS01 021A) diluted in PBS-TBSA (PBS, 0.1% [vol/vol] Triton X-100, 1 mg/ml bovine serum albumin [BSA]). The specificity of the global NifH protein antibody has been checked with Western blots by the manufacturer against a series of bacterial NifH proteins, and has, among others, predicted specificity for *Rhizobium meliloti* (Agrisera, AS01 021A). As negative controls, fixed and permeabilized tissues were incubated for 1 h with PBS-TBSA and without primary antibody (see Fig. S2 in the supplemental material). All samples were washed three times with PBST before being incubated in the dark with a goat anti-chicken IgY conjugated to Dylight 488 (Pierce, SA5-10070) for 45 min and then washed twice with PBST. Finally, the tissues were mounted in Vectashield medium containing DAPI (Vector Laboratories, H-1500) and viewed under a SP5 Leica confocal microscope with 10 \times and 63 \times objectives.

Electron microscopy. Large workers of *A. echinator* (Ae150) were dissected in 0.1 M phosphate buffer (pH 7.4), and ant digestive tracts were fixed in 2.5% glutaraldehyde (Sigma) in 0.1 M sodium cacodylate buffer (pH 7.4) for 2.5 h. This was followed by washings in the same buffer and postfixation in 1% OsO₄ for 1 h, after which samples were placed in a 1% aqueous solution of uranyl acetate and left for 12 h at 4°C. Samples were then dehydrated in an ethanol series and acetone and embedded in Agar 100 Resin (Agar Scientific Ltd.) or Spurr low-viscosity resin (Ted Pella Inc.). Ultrathin sections were stained with uranyl acetate and Reynolds lead citrate and examined with a transmission electron microscope (TEM) (JEM 100 SX [JEOL] or CM100 [FEI]).

Periodic acid-Schiff (PAS) staining. Digestive tracts from large workers of *A. octospinosus* (Ao492), taken either directly from their colony's fungus garden or after having spent 2 weeks on sterile sucrose diets, were fixed in 4% paraformaldehyde in 0.1 M phosphate buffer (pH 7.4) overnight at $+4^\circ\text{C}$ and subsequently dehydrated via a graded alcohol series and HistoClear (Sigma), followed by embedding in Paraplast Plus (Sigma). Sections were cut at 3 to 4 μ m and dried on a hot plate at 36°C. After dewaxing and rehydration, sections were treated with 1% aqueous periodic acid for 10 min, washed for 5 min in running tap water, immersed in Schiff's reagent (Sigma) for 15 min, and washed for 10 min in running tap water to develop the color. Finally, sections were dehydrated

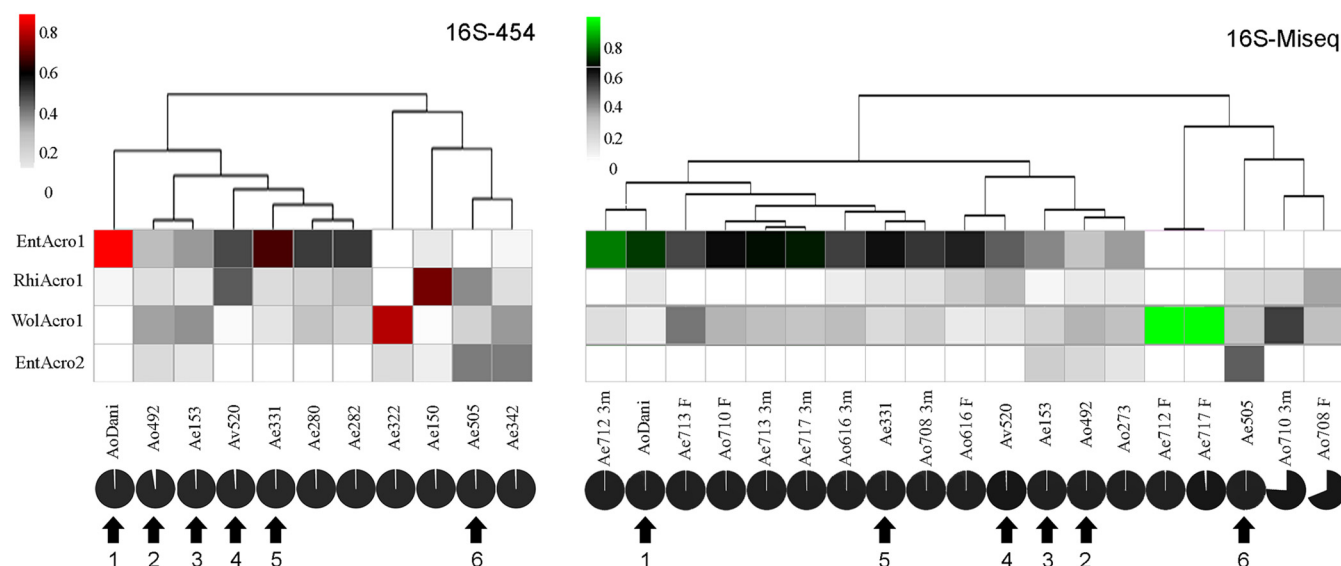


FIG 1 Combined 16S sequencing results for the gut microbiomes of sympatric colonies of *A. echinator*, *A. octospinosus*, and *A. volcanus* using both Roche 454 and Illumina Miseq 16S sequencing. OTU heat maps show the relative abundances (rarefied number of reads) of the four most abundant OTUs identified initially with 454 sequencing (see details in the text and in Table S4 in the supplemental material) in lab samples (>2 years after collection) consisting of five pooled large worker guts per colony and afterwards confirmed by Miseq sequencing of field colony samples (F) and repeated samples of these colonies 3 months after transfer to the lab (3m). From left to right, relative abundances of the 11 lab colony samples, sequenced with 454 (white, shades of gray to red heat map) and the 19 samples sequenced with Illumina Miseq (white, shades of gray to green heat map), consisting of six F plus 3m colonies, six long-term lab colonies that had already been sequenced with 454, and a new long-term lab colony sample (Ao273). We compared OTU nucleotide sequences from both runs using blastn with 100% identity and $1e-50$ E value cutoff, after which we checked whether OTUs from different platforms had identical nucleotide sequences (100%), the same classification, and the same distribution across samples (colonies) before concluding that they represented the same OTU. The top dendrograms above the heat maps segregate the microbiomes based on weighted Euclidean distances of community similarity. Pie charts at the bottom give cumulative abundances of these four OTUs (black) versus the 176 other OTUs (white) that were identified in the 454 run and the 198 other OTUs (white) that were identified in the Miseq run. The arrows and the numbers at the bottom highlight the six identical samples that were sequenced in both runs.

in ethanol and Histoclear and mounted in DPX to be viewed with a Leica DM 5000 B microscope.

Nucleotide sequence accession numbers. The sequence data have been deposited in the NCBI databases under accession numbers [SRR1956953](#) to [SRR1956970](#), [SRR1956976](#), [SRR1705540](#), [SRR1705717](#), [SRR1707353](#), [SRR1707463](#) to [SRR1707466](#), [SRR1707501](#), [SRR1707550](#), [SRR1707570](#), [SRR1707571](#), [KF613173](#), [KP256159](#) to [KP256169](#), and [KR336617](#) to [KR336619](#).

RESULTS

16S-454 and 16S-Miseq sequencing. Using a 97% sequence identity cutoff, we identified a total of 180 bacterial OTUs from the 454-pyrosequencing (see Table S4A in the supplemental material). Rarefaction curves were approaching saturation in all but one sample (Ao492), indicating that coverage was generally sufficient for community structure analyses. The four most abundant OTUs belonged to the *Mollicutes* (*Entomoplasmatales* [*EntAcro1*, and *EntAcro2*]) and *Alphaproteobacteria* (*Rhizobiales* [*RhiAcro1*] and *Wolbachia* [*WolAcro1*]) and jointly always accounted for >97% of the reads per sample (Fig. 1A; see Table S4A in the supplemental material). Although the rarefaction curve for Ao492 did not plateau (see Fig. S3A in the supplemental material), this colony also was included in the analyses because the four dominant OTUs were all present.

The ranked sample prevalences of OTUs 5 to 14 never exceeded 0.71%, while none of the other OTUs exceeded 0.07% per sample (see Table S4A in the supplemental material). *RhiAcro1* and *WolAcro1* were present in all 11 samples, and all samples had at least one of the *Entomoplasmatales* species, as

EntAcro1 was found in nine samples, *EntAcro2* was found in six samples, and five samples had both. OTU 5 was also an *Entomoplasmatales* (*EntAcro3*, found in 9 samples), but OTU 6 (*ActAcro1*) was an *Actinomycetales* (*Pseudonocardia*) that was 99% identical to one of the two vertically transmitted cuticular actinomycete symbionts (Ps1) of *A. echinator* and *A. octospinosus* (33, 46, 47). This OTU was found in the single gut sample of *A. volcanus* and in one of the two *A. octospinosus* gut samples but not in the eight *A. echinator* samples. None of the other OTUs was restricted to or specific for any of the three *Acromyrmex* ant species (see Table S4A in the supplemental material). We further characterized the *RhiAcro1*, *EntAcro1*, and *EntAcro2* OTUs using Sanger sequencing and obtained 982-bp, 1,282-bp, and 1,340-bp sequences, respectively, while the *WolAcro1* OTU has been characterized previously (48, 49). Maximum-likelihood phylogenetic trees showed that *RhiAcro1* is closely related to *Rhizobiales* strains identified in *Trachymyrmex urichii* of the attine lineage (see Fig. S4A in the supplemental material), while *EntAcro1* appeared to be closely related to *Mesoplasma lactucae* and *EntAcro2* to *Entomoplasma freundtii* (see Fig. S4B in the supplemental material).

To validate whether the overall rank order of dominant gut OTUs was independent of lab or field conditions during sampling, we sequenced a comparable set of dissected guts from field and lab colonies on a Miseq platform. Rarefaction curves were approaching saturation for all samples (see Fig. S3B in the supplemental material), indicating that coverage was sufficient for community structure analyses. *Wolbachia* was similarly dominant in *A. echinator* and *A. octospinosus* gut samples from

the field, whereas *EntAcro1* and *RhiAcro1* were abundant in field guts of *A. octospinosus* but rare in field guts of *A. echinator* (*EntAcro1* was abundant in one but <1% in two other field colonies, and *RhiAcro1* was <1% in all three field colonies). Once again, *EntAcro1*, *EntAcro2*, *WolAcro1*, and *RhiAcro1* accounted jointly for >97% of the reads per sample (Fig. 1; see Table S4B in the supplemental material), but this time there were two exceptions, Ao708(F) and Ao710(3m), that had an additional *Entomoplasmales* OTU (*EntAcro10*), in respective abundances of 31% and 24%.

The gut microbiotas of these *A. echinator* field colonies were often excessively dominated by *Wolbachia* (45.7%, 98.1%, and 99.6%) (Fig. 1) and showed consistent directional change toward *Rhizobiales* 3 months after colonies were moved to the lab to become similar to the gut microbiota of *A. octospinosus* (see Fig. S5 in the supplemental material).

Principal-coordinate analysis (PCoA) based on weighted Euclidean distances obtained from both the 454 and Miseq runs confirmed that the microbiota differed in a quantitative rather than a qualitative manner across sampling categories (Fig. 1; see Fig. S5 in the supplemental material). The relative abundances of *EntAcro1* and *EntAcro2* were significantly negatively correlated (Spearman $\rho = -0.858$; $P = 0.0007$), whereas a number of other prevalences also showed signs of positive or negative correlation (see Fig. S6 in the supplemental material) but without reaching significance. PCoA comparison of the four focal OTUs in the six samples that were sequenced on both platforms further showed that OTUs were highly reproducible in four cases and satisfactorily reproducible in the two other cases (see Fig. S5 in the supplemental material). To validate our relative abundance estimates, we performed qPCR using 16S rRNA gene-specific primers on a subset of the samples sequenced with Miseq, which showed that relative abundances obtained from the Miseq samples satisfactorily predicted the bacterial 16S rRNA gene copy numbers for *EntAcro1*, *EntAcro2*, and *RhiAcro1* (see Fig. S7 in the supplemental material).

Localization, morphology, and robustness of *Mollicutes* and *Alphaproteobacteria* against tetracycline. We designed probes specific for *Mollicutes* and *Alphaproteobacteria* OTUs (see Table S3 in the supplemental material for probe specificity details) and used fluorescent *in situ* hybridization (FISH) and confocal microscopy to examine different gut tissues of worker ants from colonies Ae150 and Ao492 (Fig. 2A). This showed that *Entomoplasmales* were present in the fat body cells (Fig. 2B) and all gut tissues (Fig. 2C, E, and F) of *A. echinator* and *A. octospinosus*: the Malpighian tubules (Fig. 2C), the ileum (Fig. 2E), and the rectum (Fig. 2F). However, *RhiAcro1* appeared to be restricted to the hindgut (ileum and rectum) (Fig. 2G and H), while *WolAcro1* was present sparsely in the hindgut (Fig. 2G) and more abundantly in the fat body cells (Fig. 2D), the latter confirming results from a previous *A. octospinosus* study (44).

We further investigated the morphology and localization of these bacteria using transmission electron microscopy (TEM) in *A. echinator*. This showed that the *Entomoplasmales* had a coccoid shape, an approximate diameter of 0.7 μm , and no bacterial cell wall (Fig. 2I and J) and that rod-shaped *Rhizobiales* could be recognized by dense cytoplasm, an average diameter of 0.4 μm , and a length range of 0.8 to 2.7 μm (Fig. 2K). *Wolbachia* was also distinct because of its typical three-layer envelope and heterogeneous cytoplasm (Fig. 2L). TEM analysis confirmed the distribution patterns that we found by FISH microscopy (Fig. 2 B to H)

and refined the resolution of the cellular localization of the bacteria. *Mollicutes* could thus be seen to occur across almost all gut tissues, both intracellularly (Fig. 2I) and extracellularly in the gut, where dividing cells could sometimes be observed (Fig. 2J), while *Rhizobiales* occurred only extracellularly in the hindgut lumen (Fig. 2G and H) and *Wolbachia* mostly intracellularly in the fat body cells (Fig. 2D), as also shown previously (44).

To assess the robustness of bacterial symbionts in and around the guts (in fat body cells and gut tissues), ants were deprived of their fungus gardens and fed on different artificial sugar diets, which showed that *WolAcro1* prevalence was not, and *RhiAcro1* prevalence was only moderately, affected by tetracycline, whereas *EntAcro1* and *EntAcro2* disappeared from all gut and fat body tissues when ants spent 28 days on such diets (see Fig. S1 in the supplemental material). We also examined the presence of bacteria in the ant fecal droplets with PCR, as the antibiotic treatment should make them disappear when free living in the gut lumen. This showed that the two *Entomoplasmales*, which are normally found in *Acromyrmex* fecal droplets, could no longer be retrieved after ants had been kept on tetracycline for 14 days, while *RhiAcro1* prevalence in fecal droplets decreased much more slowly, a decline that was mostly due to the nonfungal diet with only a minor additional effect of tetracycline (see Fig. S1 in the supplemental material). Similar patterns of decline were found in the guts, with tetracycline accelerating the disappearance of the *Entomoplasmales* species but only slightly affecting *RhiAcro1* until more than a month had passed. *Wolbachia* has previously been reported, albeit in highly variable cell numbers, from fecal droplets of both *A. echinator* and *A. octospinosus* (44, 50) and was only sporadically found in the feces of the ants that we took directly from fungus gardens or exposed to prolonged artificial sugar diets. Such diets completely eliminated *Wolbachia* from the fecal droplets but never from the gut tissues, suggesting that a fungal diet may be essential for maintaining these bacteria in the gut lumen (see Fig. S1 in the supplemental material).

NifH protein production and colocalization with *Rhizobiales* in the hindgut. Using degenerate primers, we identified multiple sequences of the *nifH* bacterial gene for nitrogenase reductase, with colony Ae342 having three such sequences (pairwise identities of 89.9%), nine other colony samples having one *nifH* sequence, and colony Ae505 having zero. A maximum-likelihood tree using these and closely related sequences showed that 10/12 sequences are closely related to *nifH* sequences originating from other *Rhizobiales* bacteria and that 2/12 sequences (18cl8_Ae342 and QC8_Ae342) are equally related to *nifH* sequences originating from both *Rhizobiales* and non-*Rhizobiales* bacteria (see Fig. S8 in the supplemental material). Using microdissections and *nifH*-specific PCR, we found in two separate experiments that *nifH* sequence signals were abundant in the hindgut but weak and irregular in the Malpighian tubules and fat body cells (Fig. 3A) and that keeping workers on a sterile sucrose solution without fungus garden food for up to 15 days maintained *nifH* genes only in the hindguts (Fig. 3A).

To investigate whether some *nifH* sequences are transcribed into active NifH proteins we performed immunofluorescence (IF) confocal microscopy with a specific anti-NifH antibody. This showed that NifH proteins were present only toward the cuticular boundaries of the ileum and rectum, where DAPI staining revealed that these NifH protein signals were localized

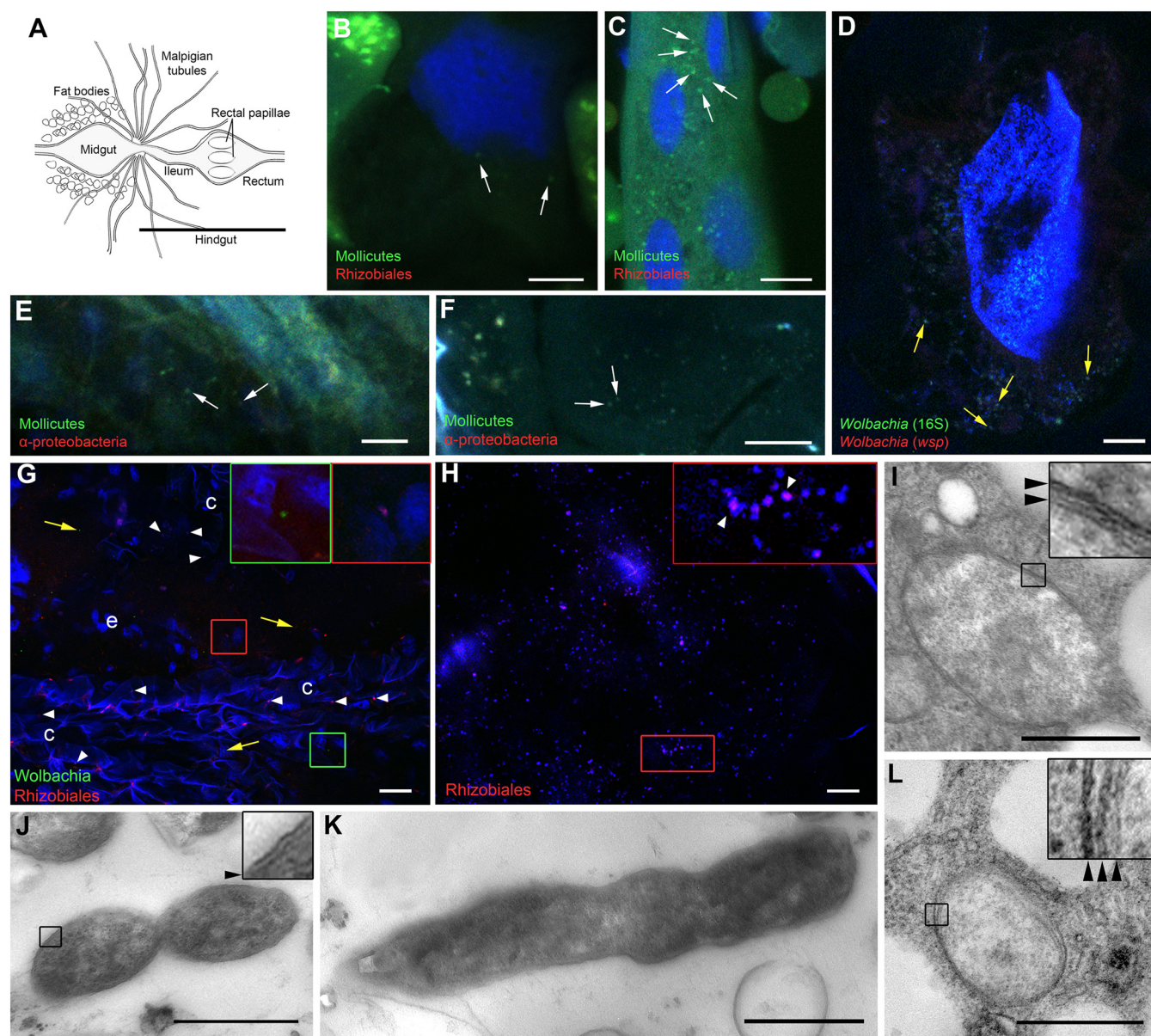


FIG 2 Distribution and structural organization of dominant bacteria in gut tissues of *Acromyrmex* leaf-cutting ants. (A) Schematic diagram of gut tissues sampled. (B and C) FISH of *Entomoplasmatales* (green, EntomA_Cy3 probe) and *Rhizobiales* (red, Phyllo_Cy5 probe) in a fat body cell (B) and a Malpighian tubule (C), showing that *Entomoplasmatales* (*Mollicutes*) are always present but *Rhizobiales* are absent. (D) *Wolbachia* (green, Wob_Cy3 and W2_Cy3 probes; red, wsp_Cy5 probe) in a fat body cell. (E and F) *Entomoplasmatales* (*Mollicutes*) (green, Entom_A488 probe) in optical sections of parts of the ileum (E) and rectum (F) where alphaproteobacteria are absent (Phyllo_Uni_Cy5 probe). (G and H) *Wolbachia* (green, Wob_Cy3 probe) and *Rhizobiales* (red, Phyllo_Cy5 probe) in other sections of the ileum (G) and rectum (H). White arrows indicate *Entomoplasmatales* (*Mollicutes*) (B to F), yellow arrows *Wolbachia* (D and G), and arrowheads *Rhizobiales* (G and H); frames in matching colors (G and H) show bacteria at higher magnification. DNA was stained with DAPI (blue). *Mollicutes* were present in almost all tissues examined (A to F), *Rhizobiales* were present only in the ileum (G) across the cuticle (marked with c), the epithelium (marked with e), and the rectum (H), and *Wolbachia* was observed only sporadically in the lumen but abundantly in the fat body cells (D and G). (I) Electron microscopy images of an *Entomoplasmatales* bacterium in a fat body cell, with the inset showing that the bacterial cell wall is lacking and black arrowheads indicating that cells are surrounded by a plasma membrane and a membrane of host origin. (J) Dividing *Entomoplasmatales* in the lumen of the rectum, with the inset showing the single plasma membrane that is characteristic of free-living *Entomoplasmatales*. (K) A rod-shaped *Rhizobiales* bacterium in the ileum. (L) A *Wolbachia* bacterium in a fat body cell, with the inset and black arrowheads showing its typical endosymbiotic three-layered envelope. Scale bars are 10 μm (B to H) and 0.5 μm (I to L). Critical interpretational images presented in this figure were also obtained for *A. octospinosus* and did not reveal any significant differences from *A. echinator*.

in or immediately next to bacterial DAPI signals (Fig. 3B). TEM confirmed that only *Rhizobiales* bacteria were localized close to the cuticle of the hindgut lumen (Fig. 3C) and that these bacteria are surrounded by a matrix that might facilitate both biofilm for-

mation and attachment to the cuticle of the rectum and ileum (Fig. 3D and E). *Rhizobiales* were most abundant in the ileum (Fig. 3E), and PAS staining of hindgut sections showed consistent red staining corresponding to abundant polysaccharides in

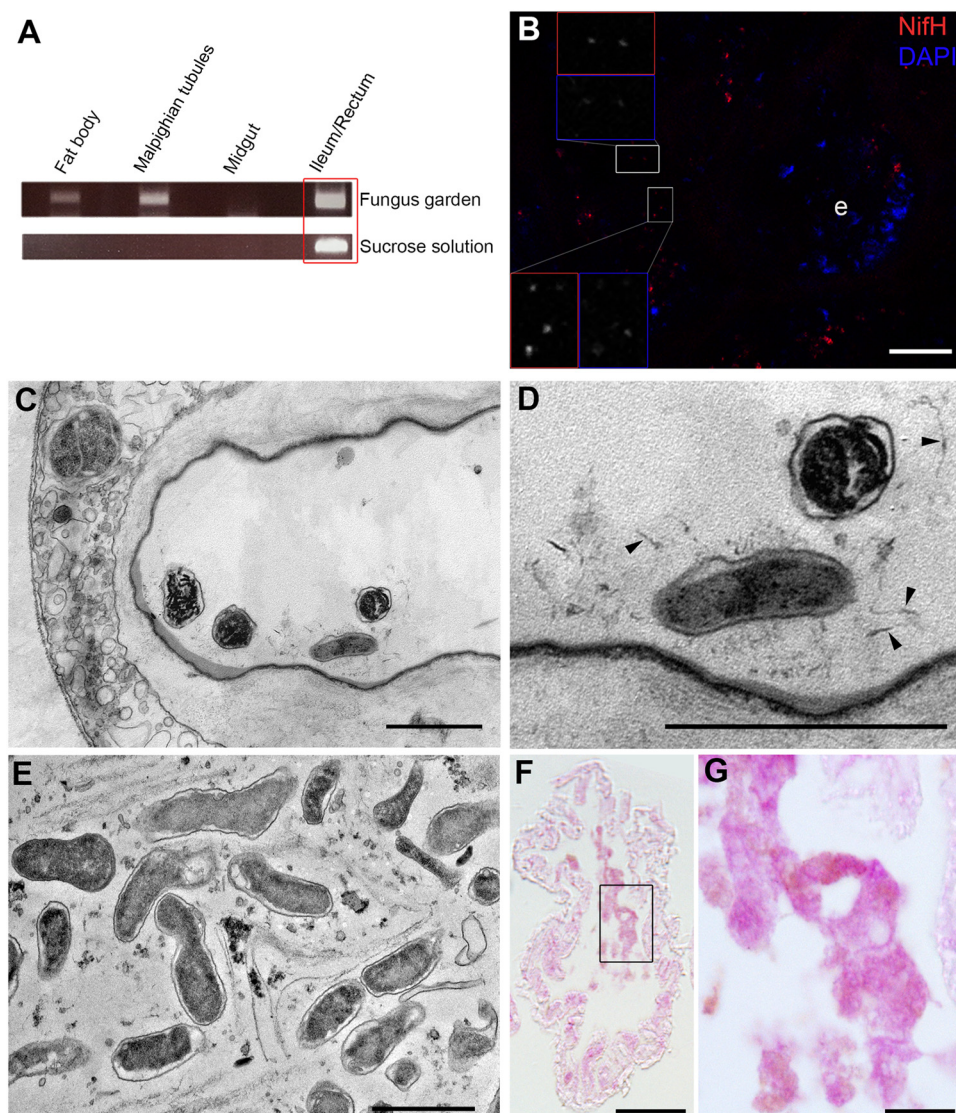


FIG 3 Presence of *Rhizobiales* bacteria and bacterial *nifH* genes and NifH proteins in the hindguts of *Acromyrmex octospinosus* leaf-cutting ant workers. (A) *nifH*-specific PCR of DNA extracted from *A. octospinosus* guts, showing weak positive signals in fat body and Malpighian tubule cells and a strong signal in the rectum/ileum, whereas only the strong rectum/ileum signal could be retrieved from ants that were kept on a sucrose diet for 15 days. All signals were confirmed to be *nifH* by Sanger sequencing and shown to be either identical or most closely related to known *nifH* sequences of *Rhizobiales* (10/12 sequences) or to give similarly close matches to both *Rhizobiales* and non-*Rhizobiales* bacteria (2/12 sequences [18cl8_Ae342 and QC8_Ae342]) (see the text for details). (B) Immunofluorescence image confirming the NifH protein (bright red dots) close to the cuticle of the ileum and covering or being directly adjacent to the bacterial DNA signals (blue dots, stained by DAPI). The host DNA of the epithelium (e) was also visible. The inset frames show magnifications of red-stained dots representing NifH and DAPI signals. (C to E) Electron microscopy image showing *Rhizobiales* bacteria close to the rectal cuticle and surrounded by a low-density matrix (C), at a higher magnification (D), and similarly in the ileum (E). (F and G) Polysaccharides detected by PAS staining in the ileums of ants kept for 2 weeks on a sterile sucrose diet without a fungus garden, showing the *Rhizobiales* biofilm at low (F) and high (G; rectangle frame in panel F) magnification. Scale bars are 10 μm (B), 1 μm (C to E), 50 μm (F), and 10 μm (G).

the matrix where the *Rhizobiales* bacteria occurred (Fig. 3F and G).

DISCUSSION

Simple gut microbiota, uniform diets, and intriguing actinomycetes. Our results matched the expectation that the gut microbiota of fungus-ingesting *Acromyrmex* leaf-cutting ants should be dominated by relatively few OTUs. A bacterial gut community dominated by few OTUs (what we refer to as “simple” here) has also been found in other eusocial insects with relatively uniform

diets, such as honeybees and bumblebees feeding on pollen and nectar (5, 28, 51) and cephalotine ants, which are mostly honeydew-collecting functional herbivores (6). Our results add yet another functionally herbivorous ant genus to the known *Rhizobiales* hosts (6, 14) but also provide novel specifications about the location and function of these gut bacteria. In particular, no other study has combined FISH, TEM, and anti-NifH IF to localize these major endosymbionts of herbivorous ants (6, 14), showing that they are compartmentalized, aided by what appears to be biofilm formation, and colocalized with bacterial NifH proteins,

whose expression is usually tightly regulated by oxygen and nitrogen levels (52).

When comparing prevalences of dominant gut bacteria in field and lab samples from the same Panamanian field site, we generally found a good correspondence (see Fig. S5 in the supplemental material), except that *RhiAcro1* and *EntAcro1* were sparse in the three *A. echinator* field colonies (see Fig. S5 and Table S4B in the supplemental material). This may be related to the habitats of *A. echinator* (open, partly sunlit areas) and *A. octospinosus* (forest) being clearly distinct and to *A. echinator* having somewhat higher fungal proteinase activity in their field fungus gardens than *A. octospinosus* (53). The natural forage of *A. echinator* colonies may thus be less nitrogen poor than the leaf fragments cut by *A. octospinosus* workers, but lab colonies of both species received the same bramble leaves (*Rubus* sp.), a type of forage that likely resembles natural *A. octospinosus* forage more than natural *A. echinator* forage. *Wolbachia* prevalences are known to differ between lab and field colonies of Panamanian *A. octospinosus*, as they significantly increase in prevalence when colonies are moved indoors, possibly due to relaxed resource constraints (44).

Our results on fungus-growing leaf-cutting ants complement recent gut microbiota studies in fungus-growing termites. These *Macrotermitinae* independently evolved farming of another basidiomycete lineage, *Termitomyces*, but retained the termite habit of predigesting wood fragments and leaf litter during a first gut passage before depositing primary feces as the substrate in which their fungal symbiont grows (54, 55). This broad diet of foraging workers and soldiers explains their complex gut microbiota (23, 56), but a resident *Macrotermes* queen was shown to have a simple gut community dominated by a single genus (*Bacillus*, >98% joint prevalence), consistent with consuming only fungal food provided by the nursing workers (23). It thus appears that substrate ingestion rather than substrate handling may be decisive for the variability of bacterial gut communities of fungus-farming eusocial insects.

Low prevalences of cuticular *Pseudonocardia* bacteria were found in the worker guts of *A. volcanus* and *A. octospinosus* (*ActAcro1*, 0.71% of the reads in Av520 and 0.38% of the reads in AoDani). Panamanian *Acromyrmex* species differ in their typical abundance of cuticular *Pseudonocardia* actinomycetes, with *A. volcanus* workers having very high coverage on their body (also in foragers), *A. octospinosus* workers having intermediate coverage, and *A. echinator* workers having the lowest coverage (reference 57 and personal observations), similar to our frequencies of detection of these bacteria in the guts (see Table S4 in the supplemental material). Further work will be needed to investigate whether the occasional presence of *ActAcro1* (99% similar to Ps1 and 97% similar to Ps2 [33]) in the guts of *Acromyrmex* species has adaptive significance or is merely due to cuticular bacteria being ingested during allogrooming.

Spatial distributions of bacterial species within the *Acromyrmex* gut. *RhiAcro1* was restricted to the hindgut, while *WolAcro1* and the *Entomoplasmatales* species were not (Fig. 2) (44). The latter two usually occur intracellularly, which apparently necessitates an extra plasma membrane of ant origin to live in the host cytoplasm (Fig. 2I, J, and L). Such extra plasma membranes have also been found in close relatives of *Entomoplasmatales* living in human reproductive organs (58) and have been hypothesized to protect bacteria against host immune defenses, a function that may also be relevant in *Wolbachia* (59, 60). The significant ten-

dency toward mutual exclusion between *EntAcro1* and *EntAcro2* suggests that similar symbionts may compete for the same niche space in the host and that complex additional interactions between the four dominant gut bacteria may exist, as *WolAcro1* had a negative effect on *EntAcro1* and *RhiAcro1* but a positive effect on *EntAcro2*. However, these correlations should be tested in larger-scale and more in-depth studies to confirm mutual exclusiveness or reinforcement.

To our knowledge, the localization of insect-associated *Rhizobiales* has been investigated in only two previous studies and only at the overall organ level: one on *Tetraponera* ants (21) and one on *Odontotaenius* beetles (12). Our TEM and PAS analyses show that *Acromyrmex* *Rhizobiales* have the characteristic rod-shaped morphology of this genus (61) and are embedded in hindgut biofilms with a polysaccharide matrix, as it has been demonstrated that the PAS reagent specifically stains polysaccharides (62). This may help these *RhiAcro1* cultures to adhere to the hindgut lining and to maintain robustness when tetracycline reduces or terminates cell divisions. The ability of proteobacteria to synthesize extracellular polysaccharides for biofilm production has previously been demonstrated in host tissues of other insects (63) and on abiotic surfaces, usually mediated by a polar adhesive that is commonly found in *Alphaproteobacteria* (64).

Putative functions of *Rhizobiales*, *Entomoplasmatales*, and *Wolbachia* in *Acromyrmex*. *RhiAcro1* and *WolAcro1* appear to be obligatorily associated with Panamanian *Acromyrmex* as symbionts, because they were present in all samples investigated (Fig. 1; see Table S4 in the supplemental material) and were impossible to remove when feeding ants sugar solutions with tetracycline (see Fig. S1 in the supplemental material). This is consistent with earlier studies showing that *Wolbachia* can survive for a month or more without proliferating (65), since a bacteriostatic antibiotic drug like tetracycline inhibits the growth but does not destroy the bacterial cells. Close relatives of *RhiAcro1* have been found in several other, mostly functionally herbivorous, ant species (6, 14, 66, 67), but *Mollicutes* (*Entomoplasmatales*), like *EntAcro1* (*Mesoplasma*) and *EntAcro2* (*Entomoplasma*), have mostly been found associated with predatory ants such as *Formica*, generalists such as *Polyrhachis*, and especially army ants, most notably in the subfamily *Aenictinae*, which are specialized predators of other ants and termites (68–70). In general, *Entomoplasmatales* are mostly intracellular pathogens and are not known to be part of biofilms, and a fairly close *Mycoplasma* relative is known to be sensitive to tetracycline (71), consistent with the rapid demise of *EntAcro1* and *EntAcro2* in our feeding experiments.

The possible function of the two *Entomoplasmatales* species remains enigmatic. Finding these bacteria intracellularly and in high cumulative abundances (see Table S4 in the supplemental material) in healthy ant colonies would appear to be incompatible with these bacteria having a direct pathological impact on their host fitness. This interpretation is consistent with no bacterial symbionts of ants having been shown so far to be virulent in the pathogenic sense, and multiple mutualistic functions having been suggested (6, 14, 70). The prevalence of *Entomoplasmatales* in several predatory ants (including army ants) and fungus-growing ants (they are also dominant in other higher attine ant species in Panama [P. Sapountzis et al., unpublished data]) suggests that their function might be somehow related to the processing of chitin, the main component of the cuticles of insect prey and fungal cell walls ingested by leaf-cutting ants, in spite of the insects pro-

ducing their own chitinases. This and the fact that *Entomoplasma* species associated with *Acromyrmex* ants vary in their potential mutual exclusiveness and correlations with *Wolbachia* abundance offer interesting questions for further research.

Rhizobiales closely related to *RhizAcro1* and other potentially nitrogen-fixing endosymbionts have been identified in several ants with protein-poor diets (6, 14, 20, 21, 32), while *Blochmania* complements the diet of *Camponotus* ants (19, 72), suggesting that these bacteria alleviate nitrogen limitation and enhance colony growth. The combination of FISH, TEM, and anti-NifH immunostaining allowed us to show that NifH proteins are indeed produced in the very same hindgut compartments where *Rhizobiales* were found, providing indications that these bacteria may actively contribute nitrogen to the symbiosis. Tissue localization data in our present study and a previous one (44) show that *Wolbachia* is abundantly present in various nonreproductive tissues and in a free-living state in the crop (foregut) of *A. octospinosus*, suggesting that it may be a mutualist with an as-yet-unknown function (44), also because no clear reproductive manipulations by *Wolbachia* infections (male killing, feminization, or cytoplasmic incompatibility) have so far been demonstrated in ants (73, 74). All four OTUs that cumulatively make up more than 97% of the *Acromyrmex* gut microbiota may thus be mutualists, but much further work will be needed to specify the metabolic networks of these bacteria and to evaluate their benefits to the fungus-farming symbiosis.

ACKNOWLEDGMENTS

Funding was provided by a Danish National Research Foundation grant (DNRF57) and an ERC Advanced Grant (323085) to J.J.B. and an Intra-European Marie Curie Fellowship to P.S. hosted by M.S. and J.J.B. (300584 GUTS FP7-PEOPLE-2011-IEF).

We thank the University of Michigan Host Microbiome Initiative (HMI) for the library preparation and advice about Miseq sequencing, the mothur forum for help with the analyses, Severine Balmand for providing the protocol for the FISH microscopy, Mette Boye and Anders Garm for access to the confocal microscope facilities, Sylvia Mathiasen, Karin Vestberg, Saria Otani, and Pepijn Kooij for lab assistance, Jelle van Zweden and David Nash for help with the statistics, Dani Moore for rearing one of the colonies, and Michael Poulsen for comments on an earlier version of the manuscript. TEM imaging data were collected at the Center for Advanced Bioimaging (CAB) Denmark, University of Copenhagen, and at the facilities of the Interinstitutional Shared Centre for Microscopic Analysis of Biological Objects, Institute of Cytology and Genetics, Siberian Branch of the Russian Academy of Sciences. The Smithsonian Tropical Research Institute in Panama made lab facilities available during fieldwork, and the Autoridad Nacional del Ambiente of Panama issued collection and export permits.

REFERENCES

- Engel P, Moran NA. 2013. The gut microbiota of insects—diversity in structure and function. *FEMS Microbiol Rev* 37:699–735. <http://dx.doi.org/10.1111/1574-6976.12025>.
- Lee W-J, Hase K. 2014. Gut microbiota-generated metabolites in animal health and disease. *Nat Chem Biol* 10:416–424. <http://dx.doi.org/10.1038/nchembio.1535>.
- Lozupone CA, Stombaugh JJ, Gordon JI, Jansson JK, Knight R. 2012. Diversity, stability and resilience of the human gut microbiota. *Nature* 489:220–230. <http://dx.doi.org/10.1038/nature11550>.
- Tremaroli V, Bäckhed F. 2012. Functional interactions between the gut microbiota and host metabolism. *Nature* 489:242–249. <http://dx.doi.org/10.1038/nature11552>.
- Koch H, Schmid-Hempel P. 2011. Bacterial communities in central European bumblebees: low diversity and high specificity. *Microb Ecol* 62: 121–133. <http://dx.doi.org/10.1007/s00248-011-9854-3>.
- Anderson KE, Russell JA, Moreau CS, Kautz S, Sullam KE, Hu Y, Basinger U, Mott BM, Buck N, Wheeler DE. 2012. Highly similar microbial communities are shared among related and trophically similar ant species. *Mol Ecol* 21:2282–2296. <http://dx.doi.org/10.1111/j.1365-294X.2011.05464.x>.
- Douglas AE. 2006. Phloem-sap feeding by animals: problems and solutions. *J Exp Bot* 57:747–754. <http://dx.doi.org/10.1093/jxb/erj067>.
- Shigenobu S, Watanabe H, Hattori M, Sakaki Y, Ishikawa H. 2000. Genome sequence of the endocellular bacterial symbiont of aphids *Buchnera* sp. *APS. Nature* 407:81–86. <http://dx.doi.org/10.1038/35024074>.
- Baumann P, Baumann L, Lai C-Y, Rouhbachsh D, Moran NA, Clark MA. 1995. Genetics, physiology, and evolutionary relationships of the genus *Buchnera*: intracellular symbionts of aphids. *Annu Rev Microbiol* 49:55–94. <http://dx.doi.org/10.1146/annurev.mi.49.100195.000415>.
- Hosokawa T, Koga R, Kikuchi Y, Meng XY, Fukatsu T. 2010. *Wolbachia* as a bacteriocyte-associated nutritional mutualist. *Proc Natl Acad Sci U S A* 107:769–774. <http://dx.doi.org/10.1073/pnas.0911476107>.
- Nikoh N, Hosokawa T, Moriyama M, Oshima K, Hattori M, Fukatsu T. 2014. Evolutionary origin of insect-*Wolbachia* nutritional mutualism. *Proc Natl Acad Sci U S A* 111:10257–10262. <http://dx.doi.org/10.1073/pnas.1409284111>.
- Ceja-Navarro JA, Nguyen NH, Karaoz U, Gross SR, Herman DJ, Andersen GL, Bruns TD, Pett-Ridge J, Blackwell M, Brodie EL. 2014. Compartmentalized microbial composition, oxygen gradients and nitrogen fixation in the gut of *Odontotaenius disjunctus*. *ISME J* 8:6–18. <http://dx.doi.org/10.1038/ismej.2013.134>.
- Sauer C, Stackebrandt E, Gadau J, Hölldobler B, Gross R. 2000. Systematic relationships and cospeciation of bacterial endosymbionts and their carpenter ant host species: proposal of the new taxon *Candidatus Blochmannia* gen. nov. *Int J Syst Evol Microbiol* 50:1877–1886.
- Russell JA, Moreau CS, Goldman-Huertas B, Fujiwara M, Lohman DJ, Pierce NE. 2009. Bacterial gut symbionts are tightly linked with the evolution of herbivory in ants. *Proc Natl Acad Sci U S A* 106:21236–21241. <http://dx.doi.org/10.1073/pnas.0907926106>.
- Hongoh Y. 2010. Diversity and genomes of uncultured microbial symbionts in the termite gut. *Biosci Biotechnol Biochem* 74:1145–1151. <http://dx.doi.org/10.1271/bbb.100094>.
- Warnecke F, Luginbühl P, Ivanova N, Ghassemian M, Richardson TH, Stege JT, Cayouette M, McHardy AC, Djordjevic G, Aboushadi N, Sorek R, Tringe SG, Podar M, Martin HG, Kunin V, Dalevi D, Madejska J, Kirton E, Platt D, Szeto E, Salamov A, Barry K, Mikhailova N, Kyrpides NC, Matson EG, Ottesen EA, Zhang X, Hernández M, Murillo C, Acosta LG, Rigoutsos I, Tamayo G, Green BD, Chang C, Rubin EM, Mathur EJ, Robertson DE, Hugenholtz P, Leadbetter JR. 2007. Metagenomic and functional analysis of hindgut microbiota of a wood-feeding higher termite. *Nature* 450:560–565. <http://dx.doi.org/10.1038/nature06269>.
- Breznak JA, Brune A. 1994. Role of microorganisms in the digestion of lignocellulose by termites. *Annu Rev Entomol* 39:453–487. <http://dx.doi.org/10.1146/annurev.en.39.010194.002321>.
- Sauer C, Dudaczek D, Hölldobler B, Gross R. 2002. Tissue localization of the endosymbiotic bacterium “*Candidatus Blochmannia floridanus*” in adults and larvae of the carpenter ant *Camponotus floridanus*. *Appl Environ Microbiol* 68:4187–4193. <http://dx.doi.org/10.1128/AEM.68.9.4187-4193.2002>.
- Feldhaar H, Straka J, Krischke M, Berthold K, Stoll S, Mueller MJ, Gross R. 2007. Nutritional upgrading for omnivorous carpenter ants by the endosymbiont *Blochmannia*. *BMC Biol* 5:48. <http://dx.doi.org/10.1186/1741-7007-5-48>.
- Stoll S, Gadau J, Gross R, Feldhaar H. 2007. Bacterial microbiota associated with ants of the genus *Tetraponera*. *Biol J Linn Soc* 90:399–412. <http://dx.doi.org/10.1111/j.1095-8312.2006.00730.x>.
- Van Borm S, Buschinger A, Boomsma JJ, Billen J. 2002. *Tetraponera* ants have gut symbionts related to nitrogen-fixing root-nodule bacteria. *Proc Biol Sci* 269:2023–2027. <http://dx.doi.org/10.1098/rspb.2002.2101>.
- Hongoh Y. 2011. Toward the functional analysis of uncultivable, symbiotic microorganisms in the termite gut. *Cell Mol Life Sci* 68:1311–1325. <http://dx.doi.org/10.1007/s00018-011-0648-z>.
- Poulsen M, Hu H, Li C, Chen Z, Xu L, Otani S, Nygaard S, Nobre T, Klaubauf S, Schindler PM, Hauser F, Pan H, Yang Z, Sonnenberg ASM, de Beer ZW, Zhang Y, Wingfield MJ, Grimmelikhuijzen CJP, de Vries RP, Korb J, Aanen DK, Wang J, Boomsma JJ, Zhang G. 2014. Complementary symbiont contributions to plant decomposition in a fungus-

- farming termite. *Proc Natl Acad Sci U S A* 111:14500–14505. <http://dx.doi.org/10.1073/pnas.1319718111>.
24. Liu N, Zhang L, Zhou H, Zhang M, Yan X, Wang Q, Long Y, Xie L, Wang S, Huang Y, Zhou Z. 2013. Metagenomic insights into metabolic capacities of the gut microbiota in a fungus-cultivating termite (*Odontotermes yunnanensis*). *PLoS One* 8:e69184. <http://dx.doi.org/10.1371/journal.pone.0069184>.
 25. Engel P, Martinson VG, Moran NA. 2012. Functional diversity within the simple gut microbiota of the honey bee. *Proc Natl Acad Sci U S A* 109:11002–11007. <http://dx.doi.org/10.1073/pnas.1202970109>.
 26. Koch H, Schmid-Hempel P. 2011. Socially transmitted gut microbiota protect bumble bees against an intestinal parasite. *Proc Natl Acad Sci U S A* 108:19288–19292. <http://dx.doi.org/10.1073/pnas.1110474108>.
 27. Kwong WK, Engel P, Koch H, Moran NA. 2014. Genomics and host specialization of honey bee and bumble bee gut symbionts. *Proc Natl Acad Sci U S A* 111:11509–11514. <http://dx.doi.org/10.1073/pnas.1405838111>.
 28. Martinson VG, Danforth BN, Minckley RL, Rueppell O, Tingek S, Moran NA. 2011. A simple and distinctive microbiota associated with honey bees and bumble bees. *Mol Ecol* 20:619–628. <http://dx.doi.org/10.1111/j.1365-294X.2010.04959.x>.
 29. Koch H, Schmid-Hempel P. 2012. Gut microbiota instead of host genotype drive the specificity in the interaction of a natural host-parasite system. *Ecol Lett* 15:1095–1103. <http://dx.doi.org/10.1111/j.1461-0248.2012.01831.x>.
 30. Campos MGR, Bogdanov S, de Almeida-Muradian LB, Szczesna T, Mancebo Y, Frigerio C, Ferreira F. 2008. Pollen composition and standardisation of analytical methods. *J Apic Res* 47:154–161. <http://dx.doi.org/10.1389/IBRA.1.47.2.12>.
 31. Quinlan RJ, Cherrett JM. 1979. The role of fungus in the diet of the leaf-cutting ant *Atta cephalotes* (L.). *Ecol Entomol* 4:151–160. <http://dx.doi.org/10.1111/j.1365-2311.1979.tb00570.x>.
 32. Pinto-Tomás AA, Anderson MA, Suen G, Stevenson DM, Chu FST, Cleland WW, Weimer PJ, Currie CR. 2009. Symbiotic nitrogen fixation in the fungus gardens of leaf-cutter ants. *Science* 326:1120–1123. <http://dx.doi.org/10.1126/science.1173036>.
 33. Andersen SB, Hansen LH, Sapountzis P, Sorensen SJ, Boomsma JJ. 2013. Specificity and stability of the *Acromyrmex-Pseudonocardia* symbiosis. *Mol Ecol* 22:4307–4321. <http://dx.doi.org/10.1111/mec.12380>.
 34. Schloss PD, Westcott SL, Ryabin T, Hall JRA, Hartmann M, Hollister EB, Lesniewski RA, Oakley BB, Parks DH, Robinson CJ, Sahl JW, Stres B, Thallinger GG, Van Horn DJ, Weber CF. 2009. Introducing mothur: open-source, platform-independent, community-supported software for describing and comparing microbial communities. *Appl Environ Microbiol* 75:7537–7541. <http://dx.doi.org/10.1128/AEM.01541-09>.
 35. Schloss PD, Gevers D, Westcott SL. 2011. Reducing the effects of PCR amplification and sequencing artifacts on 16S rRNA-based studies. *PLoS One* 6:e27310. <http://dx.doi.org/10.1371/journal.pone.0027310>.
 36. Quast C, Pruesse E, Yilmaz P, Gerken J, Schweer T, Yarza P, Peplies J, Glöckner FO. 2013. The SILVA ribosomal RNA gene database project: improved data processing and web-based tools. *Nucleic Acids Res* 41:D590–596. <http://dx.doi.org/10.1093/nar/gks1219>.
 37. Huse SM, Welch DM, Morrison HG, Sogin ML. 2010. Ironing out the wrinkles in the rare biosphere through improved OTU clustering. *Environ Microbiol* 12:1889–1898. <http://dx.doi.org/10.1111/j.1462-2920.2010.02193.x>.
 38. Kozich JJ, Westcott SL, Baxter NT, Highlander SK, Schloss PD. 2013. Development of a dual-index sequencing strategy and curation pipeline for analyzing amplicon sequence data on the MiSeq Illumina sequencing platform. *Appl Environ Microbiol* 79:5112–5120. <http://dx.doi.org/10.1128/AEM.01043-13>.
 39. Altschul SF, Gish W, Miller W, Myers EW, Lipman DJ. 1990. Basic local alignment search tool. *J Mol Biol* 215:403–410. [http://dx.doi.org/10.1016/S0022-2836\(05\)80360-2](http://dx.doi.org/10.1016/S0022-2836(05)80360-2).
 40. Drummond AJ, Ashton B, Buxton S, Cheung M, Cooper A, Duran C, Field M, Heled J, Kearse M, Markowitz S, Moir R, Stones-Havas S, Sturrock S, Thierer T, Wilson A. 2011. Geneious v5.4. Biomatters Ltd., Auckland, New Zealand.
 41. Therneau TM, Grambsch PM. 2001. Modeling survival data: extending the Cox model. Springer, New York, NY.
 42. Therneau TM. 2014. A package for survival analysis in S. R package. R Project for Statistical Computing.
 43. Braig HR, Zhou W, Dobson SL, O'Neill SL. 1998. Cloning and characterization of a gene encoding the major surface protein of the bacterial endosymbiont *Wolbachia pipientis*. *J Bacteriol* 180:2373–2378.
 44. Andersen SB, Boye M, Nash DR, Boomsma JJ. 2012. Dynamic *Wolbachia* prevalence in *Acromyrmex* leaf-cutting ants: potential for a nutritional symbiosis. *J Evol Biol* 25:1340–1350. <http://dx.doi.org/10.1111/j.1420-9101.2012.02521.x>.
 45. Lopez-Madrigal S, Balmand S, Latorre A, Heddi A, Moya A, Gil R. 2013. How does *Tremblaya princeps* get essential proteins from its nested partner *Moranella endobia* in the mealybug *Planococcus citri*? *PLoS One* 8:e77307. <http://dx.doi.org/10.1371/journal.pone.0077307>.
 46. Poulsen M, Cafaro M, Boomsma JJ, Currie CR. 2005. Specificity of the mutualistic association between actinomycete bacteria and two sympatric species of *Acromyrmex* leaf-cutting ants. *Mol Ecol* 14:3597–3604. <http://dx.doi.org/10.1111/j.1365-294X.2005.02695.x>.
 47. Seipke RF, Kaltenpoth M, Hutchings MI. 2012. *Streptomyces* as symbionts: an emerging and widespread theme? *FEMS Microbiol Rev* 36:862–876. <http://dx.doi.org/10.1111/j.1574-6976.2011.00313.x>.
 48. Van Borm S, Wenseleers T, Billen J, Boomsma JJ. 2003. Cloning and sequencing of *wsp* encoding gene fragments reveals a diversity of co-infecting *Wolbachia* strains in *Acromyrmex* leafcutter ants. *Mol Phylogenet Evol* 26:102–109. [http://dx.doi.org/10.1016/S1055-7903\(02\)00298-1](http://dx.doi.org/10.1016/S1055-7903(02)00298-1).
 49. Frost CL, Fernandez-Marin H, Smith JE, Hughes WO. 2010. Multiple gains and losses of *Wolbachia* symbionts across a tribe of fungus-growing ants. *Mol Ecol* 19:4077–4085. <http://dx.doi.org/10.1111/j.1365-294X.2010.04764.x>.
 50. Frost CL, Pollock SW, Smith JE, Hughes WOH. 2014. *Wolbachia* in the flesh: symbiont intensities in germ-line and somatic tissues challenge the conventional view of *Wolbachia* transmission routes. *PLoS One* 9:e95122. <http://dx.doi.org/10.1371/journal.pone.0095122>.
 51. Cox-Foster DL, Conlan S, Holmes EC, Palacios G, Evans JD, Moran NA, Quan P-L, Briese T, Hornig M, Geiser DM, Martinson V, vanEngelsdorp D, Kalkstein AL, Drysdale A, Hui J, Zhai J, Cui L, Hutchison SK, Simons JF, Egholm M, Pettis JS, Lipkin WI. 2007. A metagenomic survey of microbes in honey bee colony collapse disorder. *Science* 318:283–287. <http://dx.doi.org/10.1126/science.1146498>.
 52. Fischer HM. 1994. Genetic regulation of nitrogen fixation in Rhizobia. *Microbiol Rev* 58:352–386.
 53. Kooij PW, Liberti J, Giampoudakis K, Schiøtt M, Boomsma JJ. 2014. Differences in forage-acquisition and fungal enzyme activity contribute to niche segregation in Panamanian leaf-cutting ants. *PLoS One* 9:e94284. <http://dx.doi.org/10.1371/journal.pone.0094284>.
 54. Sieber R, Leuthold RH. 1981. Behavioural elements and their meaning in incipient laboratory colonies of the fungus-growing termite *Macrotermes michaelseni* (Isoptera: Macrotermitinae). *Insect Soc* 28:371–382. <http://dx.doi.org/10.1007/BF02224194>.
 55. Nobre T, Rouland-Lefèvre C, Aanen DK. 2011. Comparative biology of fungus cultivation in termites and ants, p 193–210. *In* Bignell DE, Roisin Y, Lo N (ed), *Biology of termites: a modern synthesis*. Springer, Dordrecht, Netherlands.
 56. Otani S, Mikaelyan A, Nobre T, Hansen LH, Koné NA, Sørensen SJ, Aanen DK, Boomsma JJ, Brune A, Poulsen M. 2014. Identifying the core microbial community in the gut of fungus-growing termites. *Mol Ecol* 23:4631–4644. <http://dx.doi.org/10.1111/mec.12874>.
 57. Poulsen M, Bot ANM, Currie CR, Boomsma JJ. 2002. Mutualistic bacteria and a possible trade-off between alternative defence mechanisms in *Acromyrmex* leaf-cutting ants. *Insect Soc* 49:15–19. <http://dx.doi.org/10.1007/s00040-002-8271-5>.
 58. McGowin CL, Popov VL, Pyles RB. 2009. Intracellular *Mycoplasma genitalium* infection of human vaginal and cervical epithelial cells elicits distinct patterns of inflammatory cytokine secretion and provides a possible survival niche against macrophage-mediated killing. *BMC Microbiol* 9:139. <http://dx.doi.org/10.1186/1471-2180-9-139>.
 59. Serbus LR, Casper-Lindley C, Landmann F, Sullivan W. 2008. The genetics and cell biology of *Wolbachia*-host interactions. *Annu Rev Genet* 42:683–707. <http://dx.doi.org/10.1146/annurev.genet.41.110306.130354>.
 60. Wright JD, Sjöstrand FS, Portaro JK, Barr AR. 1978. The ultrastructure of the rickettsia-like microorganism *Wolbachia pipientis* and associated virus-like bodies in the mosquito *Culex pipiens*. *J Ultrastruct Res* 63:79–85. [http://dx.doi.org/10.1016/S0022-5320\(78\)80046-X](http://dx.doi.org/10.1016/S0022-5320(78)80046-X).
 61. Kuykendall LD. 2005. Order VI. *Rhizobiales*, p 324–574. *In* Garrity G, Brenner DJ, Krieg NR, Staley JT (ed), *Bergey's manual of systematic bac-*

- teriology, vol 2. The Proteobacteria. Springer Science & Business Media, Dordrecht, Netherlands.
62. Fulcher TP, Dart JKG, McLaughlin-Borlace L, Howes R, Matheson M, Cree I. 2001. Demonstration of biofilm in infectious crystalline keratopathy using ruthenium red and electron microscopy. *Ophthalmology* 108: 1088–1092. [http://dx.doi.org/10.1016/S0161-6420\(01\)00561-9](http://dx.doi.org/10.1016/S0161-6420(01)00561-9).
 63. Kim JK, Kwon JY, Kim SK, Han SH, Won YJ, Lee JH, Kim C-H, Fukatsu T, Lee BL. 2014. Purine biosynthesis, biofilm formation, and persistence of an insect-microbe gut symbiosis. *Appl Environ Microbiol* 80:4374–4382. <http://dx.doi.org/10.1128/AEM.00739-14>.
 64. Heindl JE, Wang Y, Heckel BC, Mohari B, Feirer N, Fuqua C. 2014. Mechanisms and regulation of surface interactions and biofilm formation in *Agrobacterium*. *Plant-Microbe Interact* 5:176.
 65. Rasgon JL, Gamston CE, Ren X. 2006. Survival of *Wolbachia pipientis* in cell-free medium. *Appl Environ Microbiol* 72:6934–6937. <http://dx.doi.org/10.1128/AEM.01673-06>.
 66. Kautz S, Rubin BE, Russell JA, Moreau CS. 2013. Surveying the microbiome of ants: comparing 454 pyrosequencing with traditional methods to uncover bacterial diversity. *Appl Environ Microbiol* 79:525–534. <http://dx.doi.org/10.1128/AEM.03107-12>.
 67. Larson HK, Goffredi SK, Parra EL, Vargas O, Pinto-Tomas AA, McGlynn TP. 2014. Distribution and dietary regulation of an associated facultative Rhizobiales-related bacterium in the omnivorous giant tropical ant, *Paraponera clavata*. *Naturwissenschaften* 101:397–406. <http://dx.doi.org/10.1007/s00114-014-1168-0>.
 68. Funaro CF, Kronauer DJC, Moreau CS, Goldman-Huertas B, Pierce NE, Russell JA. 2011. Army ants harbor a host-specific clade of Entomoplasmatales bacteria. *Appl Environ Microbiol* 77:346–350. <http://dx.doi.org/10.1128/AEM.01896-10>.
 69. Johansson H, Dhaygude K, Lindström S, Helanterä H, Sundström L, Trontti K. 2013. A metatranscriptomic approach to the identification of microbiota associated with the ant *Formica exsecta*. *PLoS One* 8:e79777. <http://dx.doi.org/10.1371/journal.pone.0079777>.
 70. Kautz S, Rubin BER, Moreau CS. 2013. Bacterial infections across the ants: frequency and prevalence of *Wolbachia*, *Spiroplasma*, and *Asaia*. *Psyche J Entomol* 2013:e936341. <http://dx.doi.org/10.1155/2013/936341>.
 71. Taylor-Robinson D, Bébéar C. 1997. Antibiotic susceptibilities of mycoplasmas and treatment of mycoplasmal infections. *J Antimicrob Chemother* 40:622–630. <http://dx.doi.org/10.1093/jac/40.5.622>.
 72. De Souza DJ, Bezier A, Depoix D, Drezen JM, Lenoir A. 2009. *Blochmannia* endosymbionts improve colony growth and immune defence in the ant *Camponotus fellah*. *BMC Microbiol* 9:29. <http://dx.doi.org/10.1186/1471-2180-9-29>.
 73. Keller L, Liautard C, Reuter M, Brown WD, Sundström L, Chapuisat M. 2001. Sex ratio and *Wolbachia* infection in the ant *Formica exsecta*. *Heredity* 87:227–233. <http://dx.doi.org/10.1046/j.1365-2540.2001.00918.x>.
 74. Wenseleers T, Sundström L, Billen J. 2002. Deleterious *Wolbachia* in the ant *Formica truncorum*. *Proc R Soc B Biol Sci* 269:623–629. <http://dx.doi.org/10.1098/rspb.2001.1927>.